PERGAMON

Computers and Structures 74 (2000) 667–686

Computers & Structures

www.elsevier.com/locate/compstruc

System identification of torsionally coupled buildings

Jin-Min Ueng, Chi-Chang Lin*, Pao-Lung Lin

Department of Civil Engineering, National Chung-Hsing University, Taichung, 40227, Taiwan

Received 11 September 1997; accepted 15 February 1999

Abstract

In this study, an extended random decrement method, which considers the correlation among measurements, was employed to reduce the measured dynamic responses of general torsionally coupled multi-story building under random excitations. The Ibrahim time domain technique was then applied to calculate the modal frequencies and damping ratios based on only a few floor response measurements. To obtain the complete mode shapes, an interpolation method was developed to estimate the mode shape values for the locations without measurements. The seismic responses at floors with and without measurements were also calculated. Numerical results through a seven-story torsionally coupled building under ambient random excitations demonstrated that the proposed method is able to identify structural dominant modal parameters accurately even with highly coupled modes and noise contamination. A small number of response measurements, no requirement for input excitation measurements and simple on-line calculations make the proposed method favorable for implementation.

Keywords: System identification; Torsionally coupled building; Extended random decrement method; Ibrahim time domain technique; Earthquake engineering

1. Introduction

In recent years, system identification for structures has become an area of considerable research interest. The identified system parameters can be used to evaluate structural damage and ascertain the expected structural response to a future, different excitation. In structural control, the design of control devices requires a knowledge of the system parameters of the controlled structure. Thus, it is important that system identification be carried out in conjunction with structural control.

The system identification of torsionally coupled buildings from dynamic measurements has been rarely proposed in the literature [1,2]. Most papers discussed identification only for planar frame structures [3–6] or identified two translational and one torsional modal parameters for building structures separately [7,8]. However, buildings with nominally symmetric plans are actually asymmetric to some degree and will undergo lateral as well as torsional vibrations simultaneously when subjected to purely translational excitations. As a result of coupled lateral-torsional motions, the lateral forces experienced by various resisting elements (such as frames and shear walls, etc.) will differ from those experienced by the same elements if the building has a symmetrical plan and responds only to planar vibrations. The disregard of torsional vibration may cause an underestimation of structural responses [9]. Therefore, it is more appropriate and

* Corresponding author.

0045-7949/00/$ - see front matter
PII: S0045-7949(99)00073-5

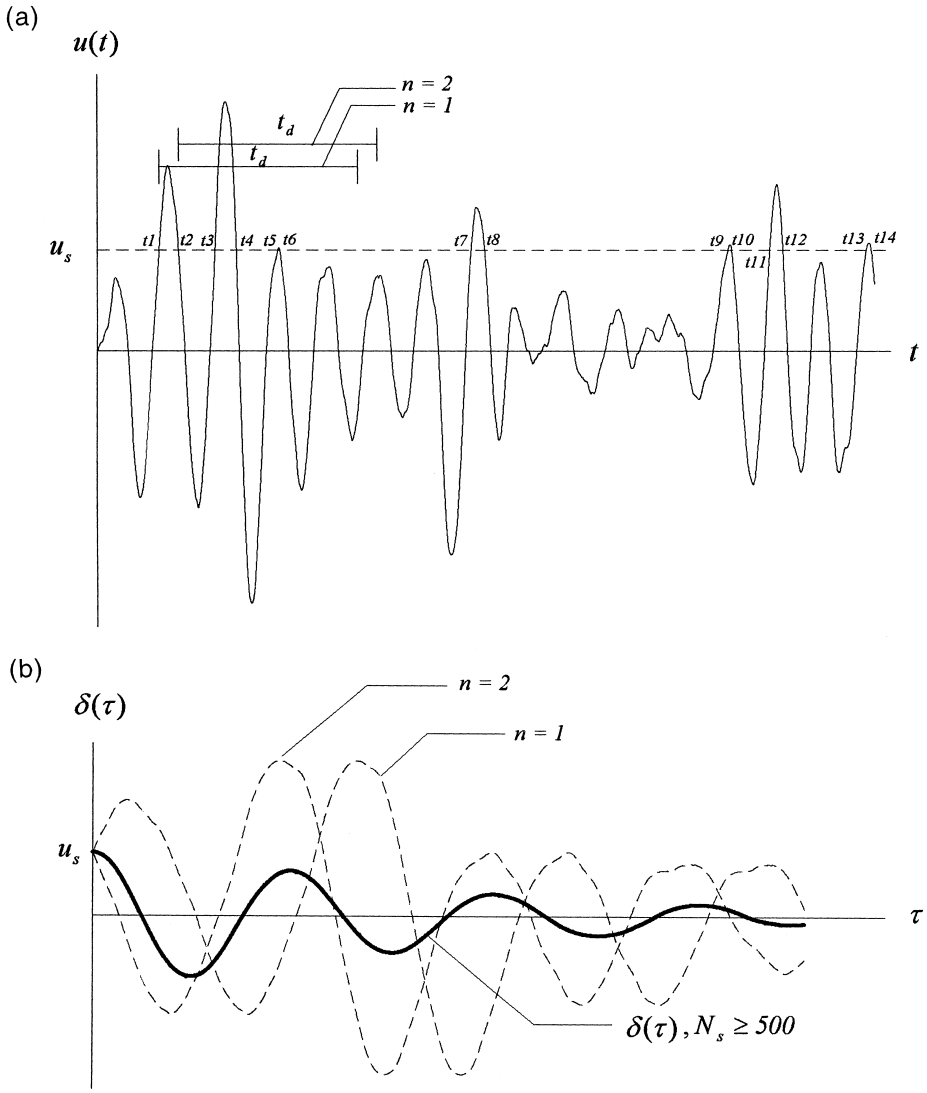

Fig. 1. (a) Response measurement and crossing times. (b) Extraction of free decay signature from response measurement.

essential to model a structure with a torsional degree of freedom.

Traditional system identification techniques require the full measurement of input excitation and its corresponding responses. However, the input excitation is generally difficult to define and accurately measure. In addition, a real structure usually possesses a large number of degrees of freedom. It is impossible and impractical to acquire full measurements because of limited number of sensors. Thus, system identification based only on response measurements at a few degrees of freedom becomes necessary from a practical point of view.

The random decrement method, originally developed by Cole [10,11] for single measurements to detect damage in aerospace structures, was commonly used for the identification of modal damping when only the response data under random excitations was available. Owing to its efficiency and simplicity in processing vibration measurements and the lack of requirement for input excitation measurements, this method is extensively applied to detect damage in civil [12] and offshore structures [13]. The identification of structural parameters from time history responses has been investigated by many researchers [14–16]. Most of the available identification techniques are mathematically complicated and sensitive to noise. Few techniques address the most critical factors such as (1) the number and the location of measurements; (2) the direction of measurements; (3) the mode coupling, and (4) the

number of modes for the response and noise levels as related to the number of degrees-of-freedom allowed in the identification model. Among these methods, the Ibrahim time domain (ITD) technique [17,18] was studied most extensively and generally accepted as the approach to solving the problem of noise contamination and the number of measurements. However, ITD technique is only applicable to free response data and emphasizes the identification of modal frequencies and damping ratios. In the case of partial measurements, only the mode shape values corresponding to the instrumented degrees-of-freedom could be obtained. To estimate the dynamic responses for the locations without measurements, the complete mode shapes should be found.

In this study, the random decrement method was modified by considering the correlation among measurements to extract the free vibration responses of a multi-story torsionally coupled building under random excitations, which lead to the identification of the building's modal frequencies, damping ratios, and mode shapes using the ITD technique. To obtain the complete mode shapes, a mode shape interpolation method was developed based on uniform shear modes and orthogonality conditions. The seismic displacement and acceleration responses for measured and unmeasured locations are also estimated. Numerical results show that the proposed method is able to identify structural dominant modal parameters and seismic responses accurately even with highly close modes and a noise-to-signal ratio of up to 20%. Small numbers of response measurements, lack of necessity for input excitation measurements and simple on-line calculations make the proposed method favorable for actual implementation.

2. Extended random decrement method

Let $u(t)$ be a response measurement (with or without noise) at a certain location in a structure, as shown in Fig. 1(a), induced by zero-mean, stationary random excitations. This time history is divided into short segments with duration t_d, which is several times the structural fundamental period. The random decrement method consists of following analysis steps to obtain a free decay response:

1. calculate an amplitude u_s, which is usually the root-mean-square value of $u(t)$;
2. select the starting time t_i for each segment such that

$$u(t_i) = u_s, \quad i = 1,2,3,\ldots$$

$$\dot{u}(t_i) \geq 0, \quad i = 1,3,5,\ldots$$

$$\dot{u}(t_i) \leq 0, \quad i = 2,4,6,\ldots$$

3. average N_s segments of the response measurement to yield a time function, $\delta(\tau)$, i.e.

$$\delta(\tau) = \frac{1}{N_s}\sum_{i=1}^{N_s} u(t_i + \tau), \quad 0 < \tau < t_d \tag{1}$$

called random decrement signature as shown in Fig. 1(b).

For a linear structure, its dynamic response can be decomposed into three parts including response due to initial displacement, initial velocity, and external loading, respectively. Following step (2) of the random decrement analysis procedure, the response due to initial velocity cancels out because parts with positive and negative initial slopes are alternatively taken and their distributions are random. In addition, since the external excitation is assumed to be a stationary random process with zero-mean, the response due to external loading also vanishes. Hence, $\delta(\tau)$ represents a free decay response due to initial displacement. Further more, the unique form of random decrement signature and the lack of requirement to input excitation measurements make the random decrement method very attractive to use for system parameter identification and damage detection.

Basically, the original random decrement method was developed to process a single measurement. For the multiple measurements taken from a real building, their correlations will be lost if the above analysis procedure is applied to each individual measurement independently. To overcome this problem, in this study, the crossing times t_i in step (2) were determined from one designated measurement. All measurements are then processed following step (3), simultaneously, to obtain their respective free decay signatures. For building structures, it is suggested that the lower floor measurement be used to determine the crossing times because it contains greater weight for the higher modes. Therefore, we can get enough number segments to superimpose in Eq. (1) in a shorter record length. This proposal was proved successful in the following numerical example.

3. Ibrahim time domain technique

The free decay response at measured station l and time t_j obtained from Eq. (1) can be expressed as the summation of m structural modes as

$$\delta_l(t_j) = x_{l,j} = \sum_{k=1}^{2m} \varphi_{lk} e^{\lambda_k t_j} \tag{2}$$

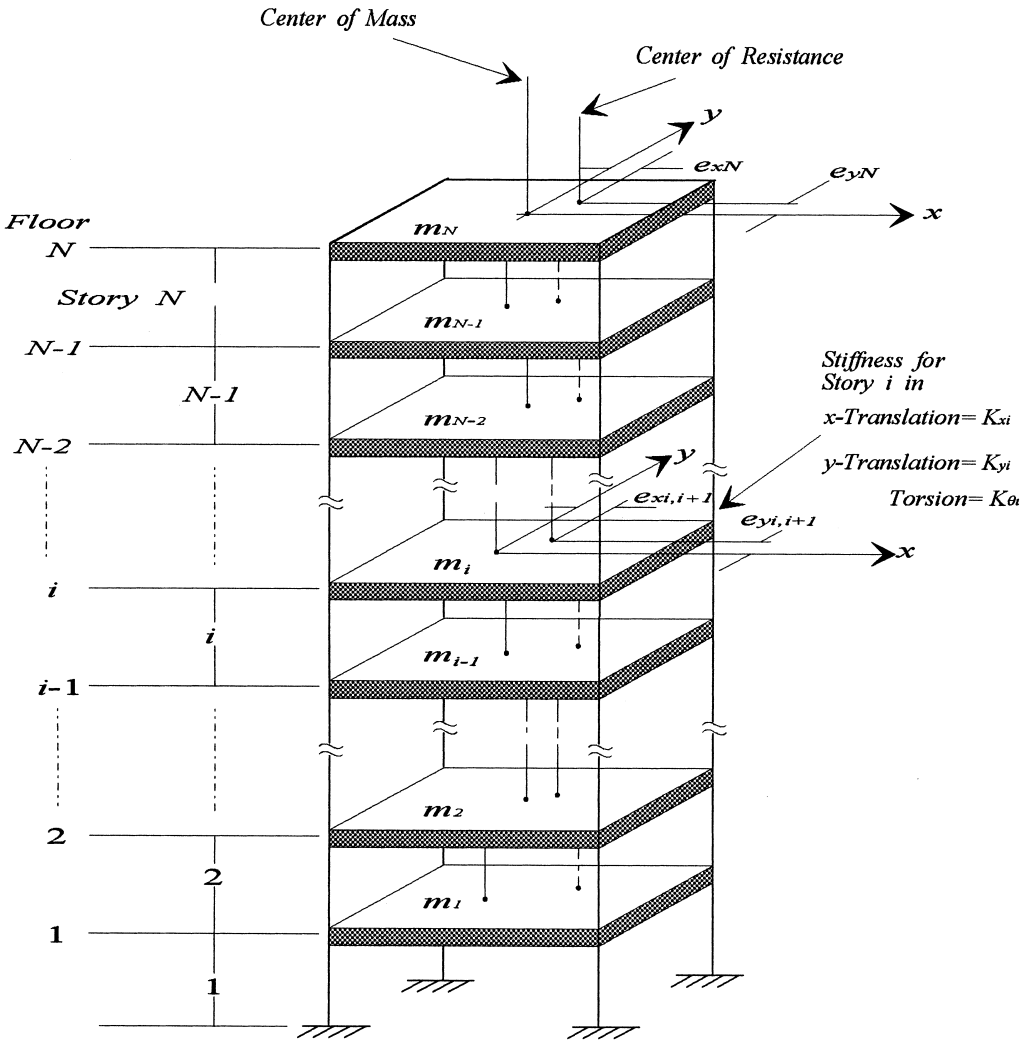

Fig. 2. N-story general torsionally coupled building.

where λ_k and φ_{lk} represent the kth complex eigenvalue and mode shape value at location l, respectively. The modal frequency ω_k and damping ratio ξ_k are then calculated using

$$\omega_k = |\lambda_k|, \qquad \xi_k = -\frac{Re(\lambda_k)}{\omega_k} \tag{3}$$

In Eq. (3), $Re(\lambda_k)$ denotes the real part of λ_k. Suppose that the responses at n different stations are measured and m modal properties are desired to be identified. We may use any m measurements for s instants (when $n \geq m$) or repeat the available measurements (when $n < m$) to construct the response matrix $\boldsymbol{X}$ using time shifting schemes [19] such that

$$\boldsymbol{X} = \boldsymbol{\Psi}\boldsymbol{\Lambda} \tag{4}$$

where

$$\boldsymbol{X} = \begin{bmatrix} x_{1,1} & x_{1,2} & \cdot & \cdot & x_{1,s} \\ x_{2,1} & x_{2,2} & \cdot & \cdot & x_{2,s} \\ \cdot & \cdot & \cdot & \cdot & \cdot \\ \cdot & \cdot & \cdot & \cdot & \cdot \\ x_{2m,1} & x_{2m,2} & \cdot & \cdot & x_{2m,s} \end{bmatrix} \tag{5a}$$

$$\boldsymbol{\Psi} = \begin{bmatrix} \varphi_{1,1} & \varphi_{1,2} & \cdot & \cdot & \varphi_{1,2m} \\ \varphi_{2,1} & \varphi_{2,2} & \cdot & \cdot & \varphi_{2,2m} \\ \cdot & \cdot & \cdot & \cdot & \cdot \\ \cdot & \cdot & \cdot & \cdot & \cdot \\ \varphi_{2m,1} & \varphi_{2m,2} & \cdot & \cdot & \varphi_{2m,2m} \end{bmatrix} \tag{5b}$$

$$\boldsymbol{\Lambda} = \begin{bmatrix} e^{\lambda_1 t_1} & e^{\lambda_1 t_2} & . & . & e^{\lambda_1 t_s} \\ e^{\lambda_2 t_1} & e^{\lambda_2 t_2} & . & . & e^{\lambda_2 t_s} \\ . & . & . & . & . \\ . & . & . & . & . \\ e^{\lambda_{2m} t_1} & e^{\lambda_{2m} t_2} & . & . & e^{\lambda_{2m} t_s} \end{bmatrix} \tag{5c}$$

Similarly, the response matrix $\hat{\boldsymbol{X}}$ corresponding to the same measured stations and Δt later in time than those in Eq. (4) can be expressed as

$$\hat{\boldsymbol{X}} = \hat{\boldsymbol{\Psi}}\boldsymbol{\Lambda} \tag{6}$$

In Eq. (6), the entries of matrices $\hat{\boldsymbol{X}}$ and $\hat{\boldsymbol{\Psi}}$ are related using

$$\hat{x}_{l,j} = \sum_{k=1}^{2m} \hat{\varphi}_{lk} e^{\lambda_k t_j}, \qquad \hat{\varphi}_{lk} = \varphi_{lk} e^{\lambda_k \Delta t} \tag{7}$$

The elimination of $\boldsymbol{\Lambda}$ from Eqs. (4) and (6) gives

$$\hat{\boldsymbol{X}} = \hat{\boldsymbol{\Psi}}\boldsymbol{\Psi}^{-1}\boldsymbol{X} = \boldsymbol{A}\boldsymbol{X} \tag{8}$$

and

$$\boldsymbol{A}\boldsymbol{\Psi} = \boldsymbol{\Psi}\boldsymbol{\alpha} \tag{9}$$

where $\boldsymbol{A}$ is defined as the $(2m \times 2m)$ system matrix. Eq. (8) is generally an over-determined system of simultaneous linear equations. The solution to obtain matrix $\boldsymbol{A}$ is not unique. Several approaches such as least square method and singular value decomposition can be used. Moreover, Eq. (9) is a standard eigenvalue equation which can be solved using any conventional method. The matrix $\boldsymbol{\alpha}$ is a diagonal matrix with entries $\alpha_k = e^{\lambda_k \Delta t}$. Let $\alpha_k = \beta_k + i\gamma_k$ and $\lambda_k = a_k + ib_k$, $(i = \sqrt{-1})$, then a_k and b_k are related to β_k and γ_k as

$$a_k = \frac{1}{2\Delta t} \ln\left(\beta_k^2 + \gamma_k^2\right) \tag{10}$$

$$b_k = \frac{1}{\Delta t} \tan^{-1}\left(\frac{\gamma_k}{\beta_k}\right) \tag{11}$$

Once the eigenvalue λ_k is obtained, the kth modal frequency and damping ratio are calculated from Eq. (3). Based on the above derivations, it is also found that the eigenvectors $\boldsymbol{\Psi}$ of matrix $\boldsymbol{A}$ are the desired complex mode shapes of the structure.

4. Torsionally coupled multi-story buildings

In reference to an ideal building consisting of rigid floors supported on massless axially inextensible columns and walls, the general torsionally coupled multi-story buildings as shown in Fig. 2 have the following features: (1) The principal axes of resistance for all of the stories are identically oriented, along the x- and y-axes shown; (2) the centers of the mass of the floors do not lie on a vertical axis; (3) the centers of resistance of the stories do not lie on a vertical axis, either, i.e. the static eccentricities at each story are not equal; (4) all floors do not have the same radius of gyration r about the vertical axis through the center of mass; and (5) ratios of the three stiffness quantities—translational stiffnesses in x and y directions, k_{xi} and k_{yi}, and torsional stiffness $k_{\theta i}$—for any story are different.

For the above general torsionally coupled N-stories building, each floor has three degrees-of-freedom: x- and y-displacements, relative to the ground, of the center of mass and rotation about a vertical axis. For floor i, they are denoted by x_i, y_i and θ_i, respectively. The undamped dynamic equations of motion for the building subjected to two horizontal ground accelerations $\ddot{x}_g(t)$ and $\ddot{y}_g(t)$, assumed to be the same at all points of the foundation, can be expressed as

$$\boldsymbol{M}\ddot{\boldsymbol{u}} + \boldsymbol{K}\boldsymbol{u} = -\boldsymbol{M}\boldsymbol{r}\ddot{u}_g \tag{12a}$$

where

$$\boldsymbol{u} = \begin{bmatrix} \boldsymbol{u}_1 \\ \boldsymbol{u}_2 \\ . \\ . \\ . \\ \boldsymbol{u}_N \end{bmatrix}, \quad \boldsymbol{r} = \begin{bmatrix} \boldsymbol{r}_1 \\ \boldsymbol{r}_2 \\ . \\ . \\ . \\ \boldsymbol{r}_N \end{bmatrix}, \quad \ddot{\boldsymbol{u}}_g = \begin{Bmatrix} \ddot{x}_g \\ \ddot{y}_g \\ 0 \end{Bmatrix},$$

$$\boldsymbol{M} = \begin{bmatrix} \boldsymbol{M}_1 & & & & \\ & \boldsymbol{M}_2 & & & \\ & & . & & \\ & & & . & \\ & & & & \boldsymbol{M}_N \end{bmatrix}$$

$$\boldsymbol{K} = \begin{bmatrix} \boldsymbol{K}_{1,1} & \boldsymbol{K}_{1,2} & & & & & & & \\ \boldsymbol{K}_{2,1} & \boldsymbol{K}_{2,2} & \boldsymbol{K}_{2,3} & & & & & & \\ & \boldsymbol{K}_{3,2} & \boldsymbol{K}_{3,3} & \boldsymbol{K}_{3,4} & & & & & \\ & & . & . & . & & & & \\ & & & . & . & . & & & \\ & & & & . & . & . & & \\ & & & & & \boldsymbol{K}_{N-1,N-2} & \boldsymbol{K}_{N-1,N-1} & \boldsymbol{K}_{N-1,N} \\ & & & & & & \boldsymbol{K}_{N,N-1} & \boldsymbol{K}_{N,N} \end{bmatrix} \tag{12b}$$

In Eq. (12b)

$$\boldsymbol{u}_i = \begin{Bmatrix} x_i \\ y_i \\ \theta_i \end{Bmatrix} \tag{13a}$$

is the displacement subvector, $\boldsymbol{r}_i = 3 \times 3$ ground influence coefficient matrix with elements of 0 and 1,

$$\boldsymbol{M}_i = \begin{bmatrix} m_i & & \\ & m_i & \\ & & I_i \end{bmatrix} \tag{13b}$$

is the mass submatrix in which m_i and I_i are lumped mass and mass moment of inertia at floor i, respectively;

$$\boldsymbol{K}_{i,i-1} = \begin{bmatrix} -k_{x_i} & 0 & k_{x_i} e_{y_{i-1,i}} \\ 0 & -k_{y_i} & -k_{y_i} e_{x_{i-1,i}} \\ & & -k_{\theta_i} \\ k_{x_i} e_{y_{i,j}} & -k_{y_i} e_{x_{i,i}} & -k_{x_i} e_{y_{i,i}} e_{y_{i-1,i}} \\ & & -k_{y_i} e_{x_{i,i}} e_{x_{i-1,i}} \end{bmatrix} \tag{13c}$$

$(i = 2, \ldots, N)$

$$\boldsymbol{K}_{i,i} = \begin{bmatrix} k_{x_i} + k_{x_{i+1}} & 0 & -k_{x_i} e_{y_{i,i}} - k_{x_{i+1}} e_{y_{i,i+1}} \\ 0 & k_{y_i} + k_{y_{i+1}} & k_{y_i} e_{x_{i,i}} + k_{y_{i+1}} e_{x_{i,i+1}} \\ & & k_{\theta_i} + k_{\theta_{i+1}} \\ -k_{x_i} e_{y_{i,i}} - k_{x_{i+1}} e_{y_{i,i+1}} & k_{y_i} e_{x_{i,i}} + k_{y_{i+1}} e_{x_{i,i+1}} & +k_{x_i} e_{y_{i,i}}^2 + k_{x_{i+1}} e_{y_{i,i+1}}^2 \\ & & +k_{y_i} e_{x_{i,i}}^2 + k_{y_{i+1}} e_{x_{i,i+1}}^2 \end{bmatrix} \quad (i = 1, \ldots, N-1) \tag{13d}$$

$$\boldsymbol{K}_{i,i} = \begin{bmatrix} k_{x_i} & 0 & -k_{x_i} e_{y_{i,i}} \\ 0 & k_{y_i} & k_{y_i} e_{x_{i,i}} \\ -k_{x_i} e_{y_{i,i}} & k_{y_i} e_{x_{i,i}} & k_{\theta_i} + k_{x_i} e_{y_{i,i}}^2 + k_{y_i} e_{x_{i,i}}^2 \end{bmatrix} \quad (i = N) \tag{13e}$$

$$\boldsymbol{K}_{i,i+1} = \begin{bmatrix} -k_{x_{i+1}} & 0 & k_{x_{i+1}} e_{y_{i+1,i+1}} \\ 0 & -k_{y_{i+1}} & -k_{y_{i+1}} e_{x_{i+1,i+1}} \\ & & -k_{\theta_{i+1}} \\ k_{x_{i+1}} e_{y_{i,i+1}} & -k_{y_{i+1}} e_{x_{i,i+1}} & -k_{x_{i+1}} e_{y_{i,i+1}} e_{y_{i+1,i+1}} \\ & & -k_{y_{i+1}} e_{x_{i,i+1}} e_{x_{i+1,i+1}} \end{bmatrix} \quad (i = 1, \ldots, N-1) \tag{13f}$$

are the stiffness submatrices, where $e_{x_{i,i}}$ and $e_{x_{i,i+1}}$ denote the static eccentricities in x-axis at floor i with respect to story i and $i+1$, respectively. The system damping will be introduced as the viscous damping ratio in each vibration mode.

After the formation of Eqs. (12a) and (12b), the building's natural frequencies and mode shapes are obtained by solving the eigenvalue problem. Because of the existence of eccentricity, the vibration modes could be highly close, leading to the difficulty in modal parameter identification.

5. Mode shape interpolation and sensor allocation

As mentioned previously, the ITD method could estimate all desired modal frequencies and damping ratios. In the case of partial measurements, only the mode shape values at the instrumented degrees-of-freedom are identified. To obtain the complete mode shapes, in this study, a mode shape interpolation method was developed to calculate the mode shape values for the locations without measurements.

For an N-story torsionally coupled structure, the jth mode shape $\boldsymbol{\Psi}_j$ is expressed as

$$\boldsymbol{\Psi}_j = \begin{bmatrix} \boldsymbol{\phi}_{xj} \\ \boldsymbol{\phi}_{yj} \\ \boldsymbol{\phi}_{\theta j} \end{bmatrix}, \quad j = 1,2,\ldots,3N \tag{14}$$

where $\boldsymbol{\phi}_{xj}$, $\boldsymbol{\phi}_{yj}$ and $\boldsymbol{\phi}_{\theta j}$ denote its components in the x, y and θ directions. It is reasonably assumed that the $\boldsymbol{\phi}_{xj}$, $\boldsymbol{\phi}_{yj}$ and $\boldsymbol{\phi}_{\theta j}$ of any torsionally coupled building are the linear combination of the shear mode shapes, $\boldsymbol{\varphi}_j$, of its corresponding N-story uncoupled (or say planar) system with the same mass distribution and uniform stiffness along the height. Then, we can form a set of functions $(\boldsymbol{\varphi}_1 - \boldsymbol{\varphi}_2)$, $(\boldsymbol{\varphi}_1 - \boldsymbol{\varphi}_3)$, $(\boldsymbol{\varphi}_1 - \boldsymbol{\varphi}_4), \ldots,$ $(\boldsymbol{\varphi}_1 - \boldsymbol{\varphi}_N)$ as the basic ingredients for mode shape interpolation. Let p $(p \geq 2)$ be the number of floors where the vibration responses in x-, y- and θ-direction are measured. Then, the mode shape interpolation formulae for all $3N$ mode shapes in d-direction ($d = x, y,$ or θ) are expressed as

$$\boldsymbol{\phi}_{d,j} = a_{d,j1}\boldsymbol{\varphi}_1 + \sum_{b=2}^{p+\mathrm{int}((j-1)/3)} a_{d,jb}(\boldsymbol{\varphi}_1 - \boldsymbol{\varphi}_b), \quad j = 1,2,\ldots,(N-p+1)\times 3 \tag{15a}$$

$$\boldsymbol{\phi}_{d,j} = a_{d,j1}\boldsymbol{\varphi}_1 + \sum_{b=2}^{N} a_{d,jb}(\boldsymbol{\varphi}_1 - \boldsymbol{\varphi}_b), \quad j = (N-p+1)\times 3 + 1, \ldots, 3N \tag{15b}$$

where int(-) indicates the integer part of the number in parenthesis. $a_{d,j1}$ and $a_{d,jb}$ are constant coefficients to be determined by the identified mode shape values and

orthogonality conditions among the modes. For instance, for a seven-story ($N = 7$) torsionally coupled building in which three floors ($p = 3$) are measured, the first three mode shapes are expressed as

$$\begin{aligned}\boldsymbol{\phi}_{x,1} &= a_{x,11}\boldsymbol{\varphi}_1 + a_{x,12}(\boldsymbol{\varphi}_1 - \boldsymbol{\varphi}_2) + a_{x,13}(\boldsymbol{\varphi}_1 - \boldsymbol{\varphi}_3)\\ \boldsymbol{\phi}_{y,1} &= a_{y,11}\boldsymbol{\varphi}_1 + a_{y,12}(\boldsymbol{\varphi}_1 - \boldsymbol{\varphi}_2) + a_{y,13}(\boldsymbol{\varphi}_1 - \boldsymbol{\varphi}_3)\\ \boldsymbol{\phi}_{\theta,1} &= a_{\theta,11}\boldsymbol{\varphi}_1 + a_{\theta,12}(\boldsymbol{\varphi}_1 - \boldsymbol{\varphi}_2) + a_{\theta,13}(\boldsymbol{\varphi}_1 - \boldsymbol{\varphi}_3)\end{aligned} \tag{16a}$$

$$\begin{aligned}\boldsymbol{\phi}_{x,2} &= a_{x,21}\boldsymbol{\varphi}_1 + a_{x,22}(\boldsymbol{\varphi}_1 - \boldsymbol{\varphi}_2) + a_{x,23}(\boldsymbol{\varphi}_1 - \boldsymbol{\varphi}_3)\\ \boldsymbol{\phi}_{y,2} &= a_{y,21}\boldsymbol{\varphi}_1 + a_{y,22}(\boldsymbol{\varphi}_1 - \boldsymbol{\varphi}_2) + a_{y,23}(\boldsymbol{\varphi}_1 - \boldsymbol{\varphi}_3)\\ \boldsymbol{\phi}_{\theta,2} &= a_{\theta,21}\boldsymbol{\varphi}_1 + a_{\theta,22}(\boldsymbol{\varphi}_1 - \boldsymbol{\varphi}_2) + a_{\theta,23}(\boldsymbol{\varphi}_1 - \boldsymbol{\varphi}_3)\end{aligned} \tag{16b}$$

$$\begin{aligned}\boldsymbol{\phi}_{x,3} &= a_{x,31}\boldsymbol{\varphi}_1 + a_{x,32}(\boldsymbol{\varphi}_1 - \boldsymbol{\varphi}_2) + a_{x,33}(\boldsymbol{\varphi}_1 - \boldsymbol{\varphi}_3)\\ \boldsymbol{\phi}_{y,3} &= a_{y,31}\boldsymbol{\varphi}_1 + a_{y,32}(\boldsymbol{\varphi}_1 - \boldsymbol{\varphi}_2) + a_{y,33}(\boldsymbol{\varphi}_1 - \boldsymbol{\varphi}_3)\\ \boldsymbol{\phi}_{\theta,3} &= a_{\theta,31}\boldsymbol{\varphi}_1 + a_{\theta,32}(\boldsymbol{\varphi}_1 - \boldsymbol{\varphi}_2) + a_{\theta,33}(\boldsymbol{\varphi}_1 - \boldsymbol{\varphi}_3)\end{aligned} \tag{16c}$$

Similarly, the 4th to 12th mode shapes are expressed as

$$\begin{aligned}\boldsymbol{\phi}_{d,4} &= a_{d,41}\boldsymbol{\varphi}_1 + a_{d,42}(\boldsymbol{\varphi}_1 - \boldsymbol{\varphi}_2) + a_{d,43}(\boldsymbol{\varphi}_1 - \boldsymbol{\varphi}_3)\\ &\quad + a_{d,44}(\boldsymbol{\varphi}_1 - \boldsymbol{\varphi}_4)\end{aligned} \tag{17a}$$

$$\begin{aligned}\boldsymbol{\phi}_{d,5} &= a_{d,51}\boldsymbol{\varphi}_1 + a_{d,52}(\boldsymbol{\varphi}_1 - \boldsymbol{\varphi}_2) + a_{d,53}(\boldsymbol{\varphi}_1 - \boldsymbol{\varphi}_3)\\ &\quad + a_{d,54}(\boldsymbol{\varphi}_1 - \boldsymbol{\varphi}_4)\end{aligned} \tag{17b}$$

$$\begin{aligned}\boldsymbol{\phi}_{d,6} &= a_{d,61}\boldsymbol{\varphi}_1 + a_{d,62}(\boldsymbol{\varphi}_1 - \boldsymbol{\varphi}_2) + a_{d,63}(\boldsymbol{\varphi}_1 - \boldsymbol{\varphi}_3)\\ &\quad + a_{d,64}(\boldsymbol{\varphi}_1 - \boldsymbol{\varphi}_4)\end{aligned} \tag{17c}$$

$$\begin{aligned}\boldsymbol{\phi}_{d,7} &= a_{d,71}\boldsymbol{\varphi}_1 + a_{d,72}(\boldsymbol{\varphi}_1 - \boldsymbol{\varphi}_2) + a_{d,73}(\boldsymbol{\varphi}_1 - \boldsymbol{\varphi}_3)\\ &\quad + a_{d,74}(\boldsymbol{\varphi}_1 - \boldsymbol{\varphi}_4) + a_{d,75}(\boldsymbol{\varphi}_1 - \boldsymbol{\varphi}_5)\end{aligned} \tag{18a}$$

$$\begin{aligned}\boldsymbol{\phi}_{d,8} &= a_{d,81}\boldsymbol{\varphi}_1 + a_{d,82}(\boldsymbol{\varphi}_1 - \boldsymbol{\varphi}_2) + a_{d,83}(\boldsymbol{\varphi}_1 - \boldsymbol{\varphi}_3)\\ &\quad + a_{d,84}(\boldsymbol{\varphi}_1 - \boldsymbol{\varphi}_4) + a_{d,85}(\boldsymbol{\varphi}_1 - \boldsymbol{\varphi}_5)\end{aligned} \tag{18b}$$

$$\begin{aligned}\boldsymbol{\phi}_{d,9} &= a_{d,91}\boldsymbol{\varphi}_1 + a_{d,92}(\boldsymbol{\varphi}_1 - \boldsymbol{\varphi}_2) + a_{d,93}(\boldsymbol{\varphi}_1 - \boldsymbol{\varphi}_3)\\ &\quad + a_{d,94}(\boldsymbol{\varphi}_1 - \boldsymbol{\varphi}_4) + a_{d,95}(\boldsymbol{\varphi}_1 - \boldsymbol{\varphi}_5)\end{aligned} \tag{18c}$$

$$\begin{aligned}\boldsymbol{\phi}_{d,10} &= a_{d,101}\boldsymbol{\varphi}_1 + a_{d,102}(\boldsymbol{\varphi}_1 - \boldsymbol{\varphi}_2)\\ &\quad + a_{d,103}(\boldsymbol{\varphi}_1 - \boldsymbol{\varphi}_3) + a_{d,104}(\boldsymbol{\varphi}_1 - \boldsymbol{\varphi}_4)\\ &\quad + a_{d,105}(\boldsymbol{\varphi}_1 - \boldsymbol{\varphi}_5) + a_{d,106}(\boldsymbol{\varphi}_1 - \boldsymbol{\varphi}_6)\end{aligned} \tag{19a}$$

$$\begin{aligned}\boldsymbol{\phi}_{d,11} &= a_{d,111}\boldsymbol{\varphi}_1 + a_{d,112}(\boldsymbol{\varphi}_1 - \boldsymbol{\varphi}_2)\\ &\quad + a_{d,113}(\boldsymbol{\varphi}_1 - \boldsymbol{\varphi}_3) + a_{d,114}(\boldsymbol{\varphi}_1 - \boldsymbol{\varphi}_4)\\ &\quad + a_{d,115}(\boldsymbol{\varphi}_1 - \boldsymbol{\varphi}_5) + a_{d,116}(\boldsymbol{\varphi}_1 - \boldsymbol{\varphi}_6)\end{aligned} \tag{19b}$$

$$\begin{aligned}\boldsymbol{\phi}_{d,12} &= a_{d,121}\boldsymbol{\varphi}_1 + a_{d,122}(\boldsymbol{\varphi}_1 - \boldsymbol{\varphi}_2)\\ &\quad + a_{d,123}(\boldsymbol{\varphi}_1 - \boldsymbol{\varphi}_3) + a_{d,124}(\boldsymbol{\varphi}_1 - \boldsymbol{\varphi}_4)\\ &\quad + a_{d,125}(\boldsymbol{\varphi}_1 - \boldsymbol{\varphi}_5) + a_{d,126}(\boldsymbol{\varphi}_1 - \boldsymbol{\varphi}_6)\end{aligned} \tag{19c}$$

and finally, the 13th–21st mode shapes are expressed in terms of all of the basis ingredients

$$\begin{aligned}\boldsymbol{\phi}_{d,j} &= a_{d,j1}\boldsymbol{\varphi}_1 + a_{d,j2}(\boldsymbol{\varphi}_1 - \boldsymbol{\varphi}_2) + a_{d,j3}(\boldsymbol{\varphi}_1 - \boldsymbol{\varphi}_3)\\ &\quad + a_{d,j4}(\boldsymbol{\varphi}_1 - \boldsymbol{\varphi}_4) + a_{d,j5}(\boldsymbol{\varphi}_1 - \boldsymbol{\varphi}_5)\\ &\quad + a_{d,j6}(\boldsymbol{\varphi}_1 - \boldsymbol{\varphi}_6) + a_{d,j7}(\boldsymbol{\varphi}_1 - \boldsymbol{\varphi}_7)\\ j &= 13,14,\ldots,21\end{aligned} \tag{20}$$

As we can see from Eqs. (16a)–(16c), in the first three mode shape interpolation formulae, there are nine unknown constant coefficients, $a_{d,j1}$ and $a_{d,jb}$, which can be determined by the nine identified mode shape values at the three measured floors in three directions and double-checked by the orthogonality conditions among the first three modes. In the fourth mode shape interpolation formulae of Eq. (17a), there are 12 unknowns. They are again determined using the nine identified mode shape values and three orthogonality conditions between the fourth and the identified first three modes. So are the same calculation procedures for the remaining modes. Finally, the fourth to sixth mode shapes are modified using the orthogonality conditions among themselves. It has been verified that with any p ($p \geq 2$) measured floors ($3p$ response measurements), there are always enough conditions to determine the unknown coefficients. This proves that the proposed mode shape interpolation method is feasible.

It is obvious that the number and location of the measurements will affect the accuracy of the parameter identification. The more floor responses measured, the more accurate the modal parameters obtained. For a high-rise building, it is suggested that at least three floor responses (at low, medium and top floor, respectively) be measured. Then, using the proposed mode shape interpolation technique, we can obtain the complete dominant mode shapes accurately. In particular, for a class of regular torsionally coupled buildings which have the same geometry in plan and the same locations for columns and shear walls, their modal frequencies and mode shapes may be determined by analyzing the modal parameters of their corresponding

Table 1
System properties of example seven-story torsionally coupled building

Floor i	Mass m_i (kg)	Inertia, I_i (kg/m^2)	C.M. (x_i,y_i) (m)	Story, i	k_{x_i} (N/m)	k_{y_i} (N/m)	$k_{\theta_i}M$ (N/m)	C.R. (x_i,y_i) (m)
1	2.0×10^5	1.28×10^7	(1.0,1.0)	1	9.0×10^8	8.5×10^8	5.0×10^{10}	(4.0,4.0)
2	2.0×10^5	1.28×10^7	(1.0,1.0)	2	9.0×10^8	8.5×10^8	5.0×10^{10}	(4.0,4.0)
3	2.0×10^5	1.28×10^7	(1.0,1.0)	3	9.0×10^8	8.5×10^8	5.0×10^{10}	(4.0,4.0)
4	1.9×10^5	1.07×10^7	(0.8,0.9)	4	8.5×10^8	7.5×10^8	4.5×10^{10}	(3.2,3.0)
5	1.9×10^5	1.07×10^7	(0.8,0.9)	5	8.5×10^8	7.5×10^8	4.5×10^{10}	(3.2,3.0)
6	1.9×10^5	1.07×10^7	(0.8,0.9)	6	8.5×10^8	7.5×10^8	4.5×10^{10}	(3.2,3.0)
7	1.8×10^5	8.82×10^6	(0.8,0.9)	7	8.0×10^8	7.0×10^8	4.0×10^{10}	(2.8,2.9)

torsionally uncoupled systems and an associated one-story torsionally coupled system [20,21]. For such a regular torsionally coupled building, the number of sensors can be further reduced. It has been demonstrated [22] that only three sensors instrumented at the low, medium and top floors to measure either x or y translations, and another three sensors installed at a certain lower floor to measure its x, y and θ responses are enough to calculate the complete modal parameters of the torsionally coupled system.

6. Numerical verifications

A seven-story ($N=7$) general torsionally coupled building is presented to demonstrate the efficacy of the proposed mode shape interpolation technique and modal parameter identification procedure. The system properties of the model structure are given in Table 1. First of all, to verify the mode shape interpolation method, assumed that the mode shape values in 1F, 4F, 7F (case 1) and 1F, 7F (case 2) are known. The complete first six mode shapes calculated using Eqs. (15a) and (15b) for both cases are shown in Fig. 3. There are very good agreement between the calculated and the true mode shapes even with a minimum number of known floor values as in case 2. This indicates the accuracy and efficacy of Eqs. (15a) and (15b). In Fig. 3, case 1 has better results than case 2, as expected.

Rayleigh damping is assumed for the first and second modal damping ratios $\xi_1=\xi_2=5\%$ to generate the floor responses. Then, we consider that the system properties are unknown and carry out the identification procedure. Two cases, noise-free and random noise [23] with noise-to-signal ratio (NSR) equal to 20%, are studied to investigate the sensitivity of noise level to the identification accuracy. For all floor response measurements, the complete modal parameters can be identified even with noise contamination. Again, two cases of partial floor measurements at 1F, 3F, 5F, 7F (case 1) and at 1F, 4F, 7F (case 2) are studied to investigate the effect of the number of measurements on the identification accuracy. Fig. 4 shows the response measurements at 1F, 4F, 7F in x, y and θ directions for NSR = 20% under a random environmental load. The corresponding free decay responses extracted by the extended random decrement method are shown in Fig. 4 The first six identified modal frequencies and damping ratios using the ITD method versus the actual ones for both cases with different noise levels are given in Table 2. It is found that for

Table 2
Identified modal frequencies and damping ratios

Mode no.	Natural frequency (Hz)					Damping ratio (%)				
	True	NSR = 0%		NSR = 20%		True	NSR = 0%		NSR = 20%	
		Case 1	Case 2	Case 1	Case 2		Case 1	Case 2	Case 1	Case 2
1	1.718	1.720	1.725	1.712	1.712	5.00	5.06	5.06	4.71	4.83
2	2.234	2.238	2.243	2.243	2.244	5.00	5.47	5.73	4.14	3.93
3	2.926	2.927	2.933	2.944	2.930	5.36	5.39	5.49	6.60	5.84
4	5.049	4.945	4.970	5.157	5.138	7.35	5.26	3.83	1.43	1.57
5	6.407	6.340	6.310	6.166	6.130	8.86	2.62	ni[a]	4.20	ni[a]
6	7.936	7.696	ni[a]	ni[a]	ni[a]	10.65	0.49	ni[a]	ni[a]	ni[a]

[a] ni: Not identified.

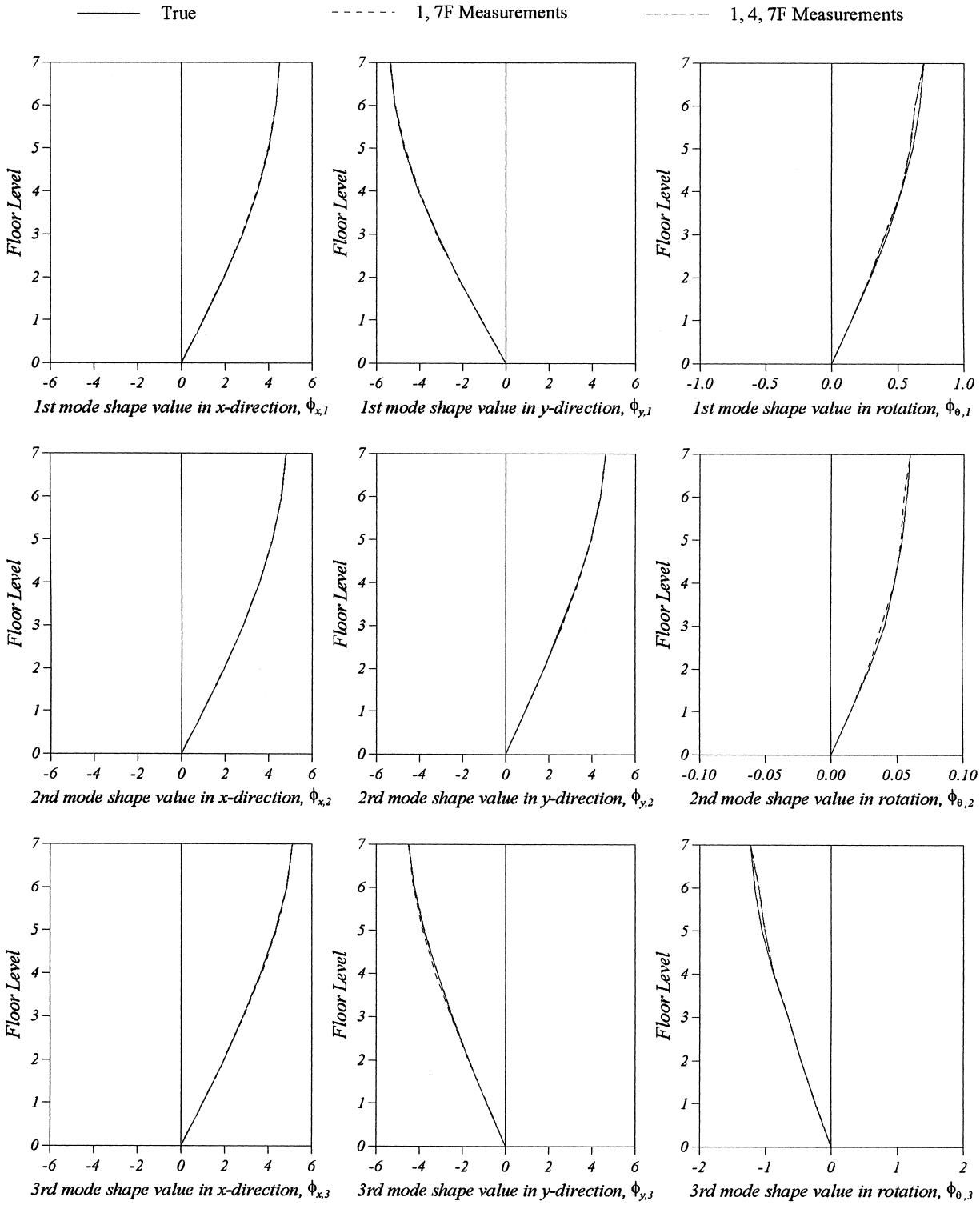

Fig. 3. Calculated vs. true mode shapes of example torsionally coupled building.

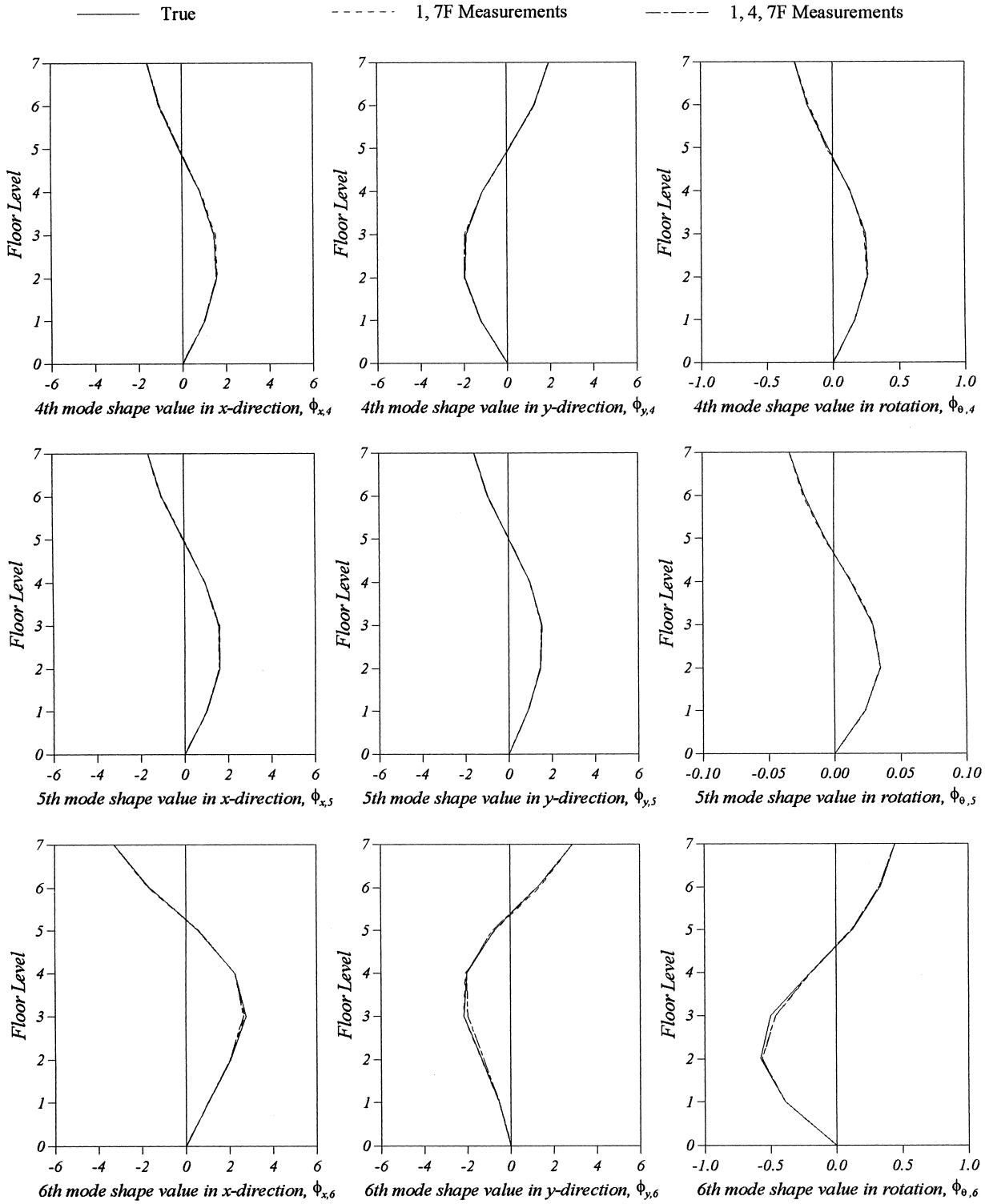

Fig. 3 (*continued*)

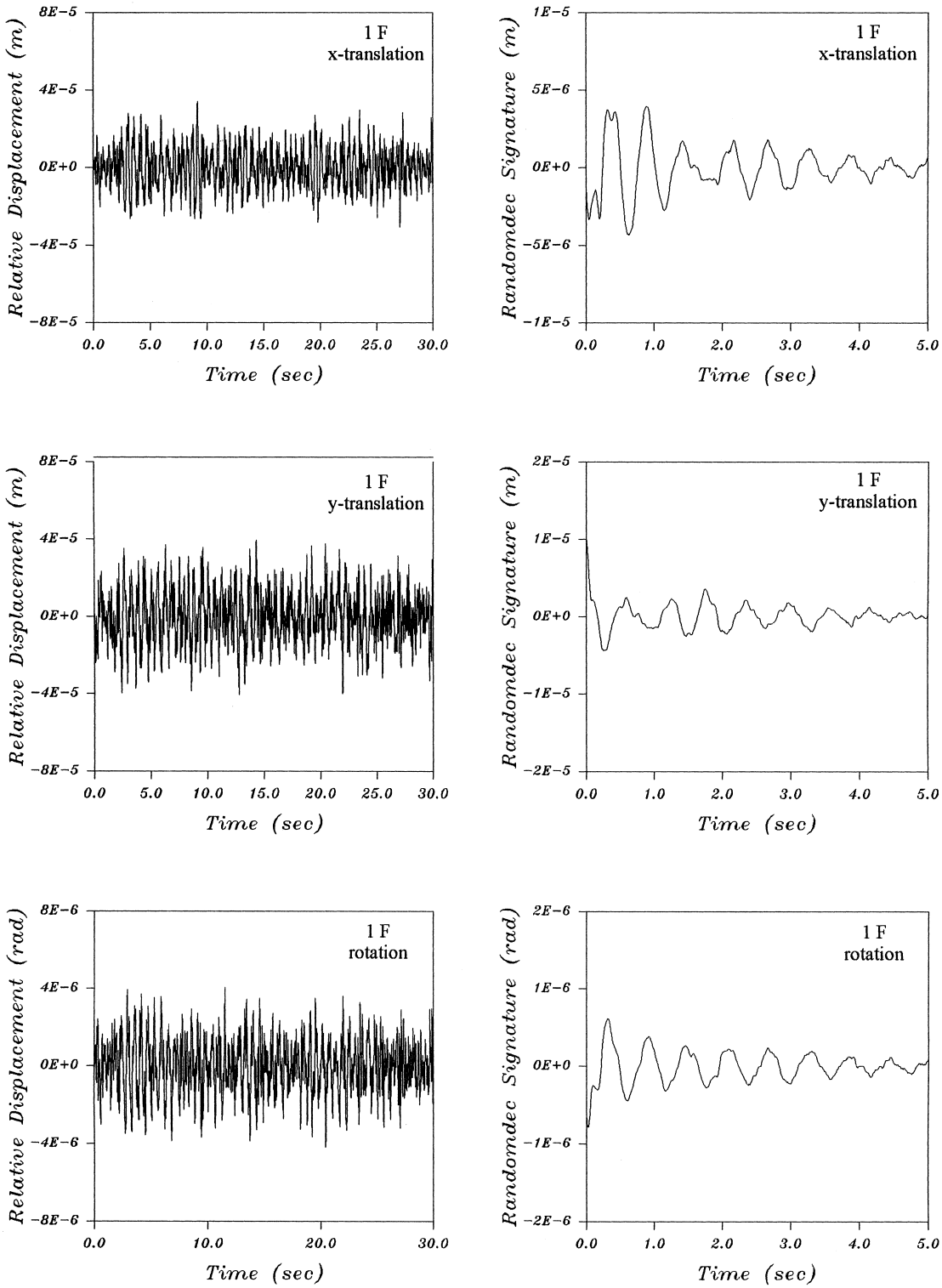

Fig. 4. Response measurements and free decay response at 1F, 4F and 7F in x, y, θ directions (NSR = 20%).

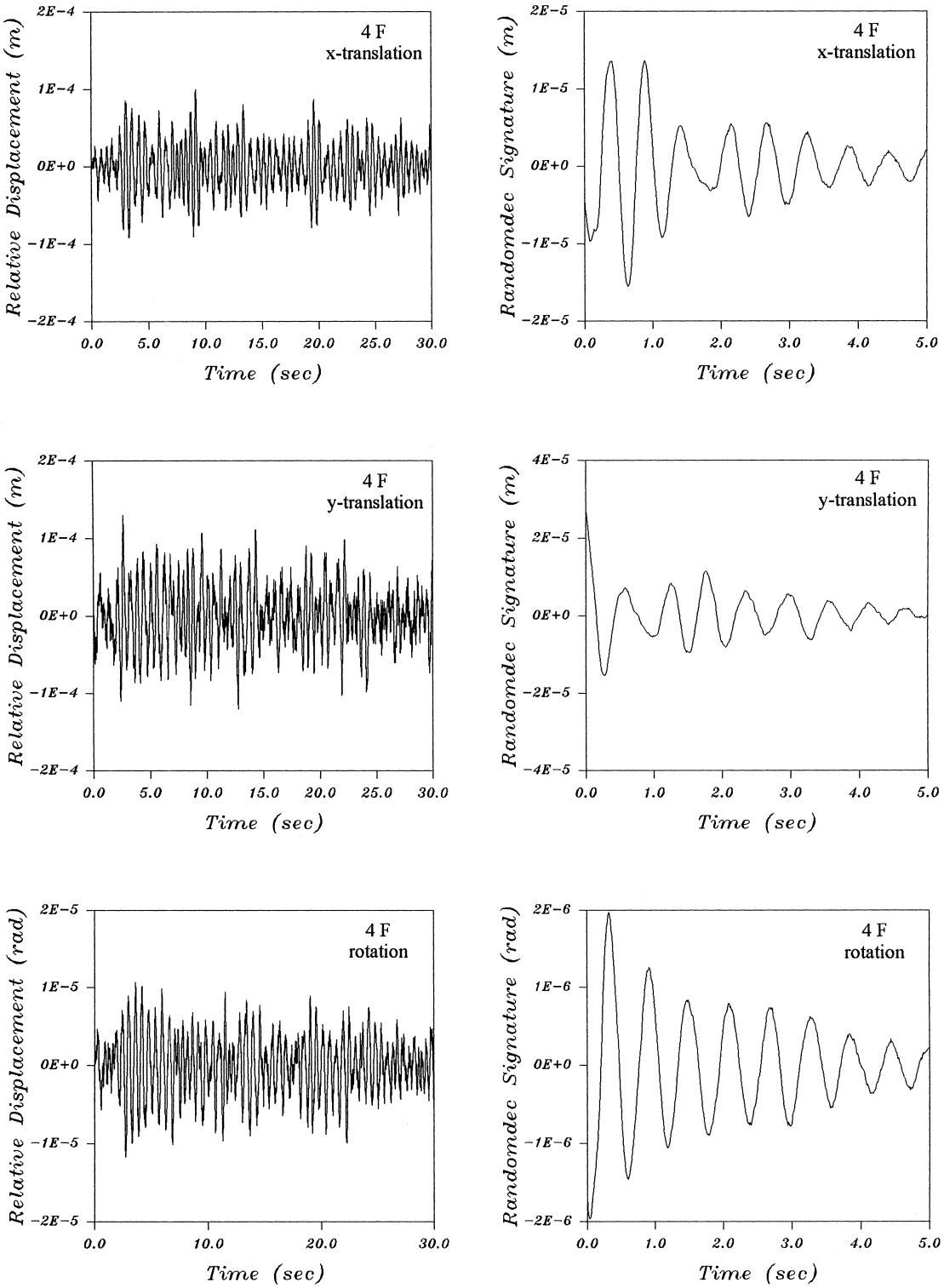

Fig. 4 (*continued*)

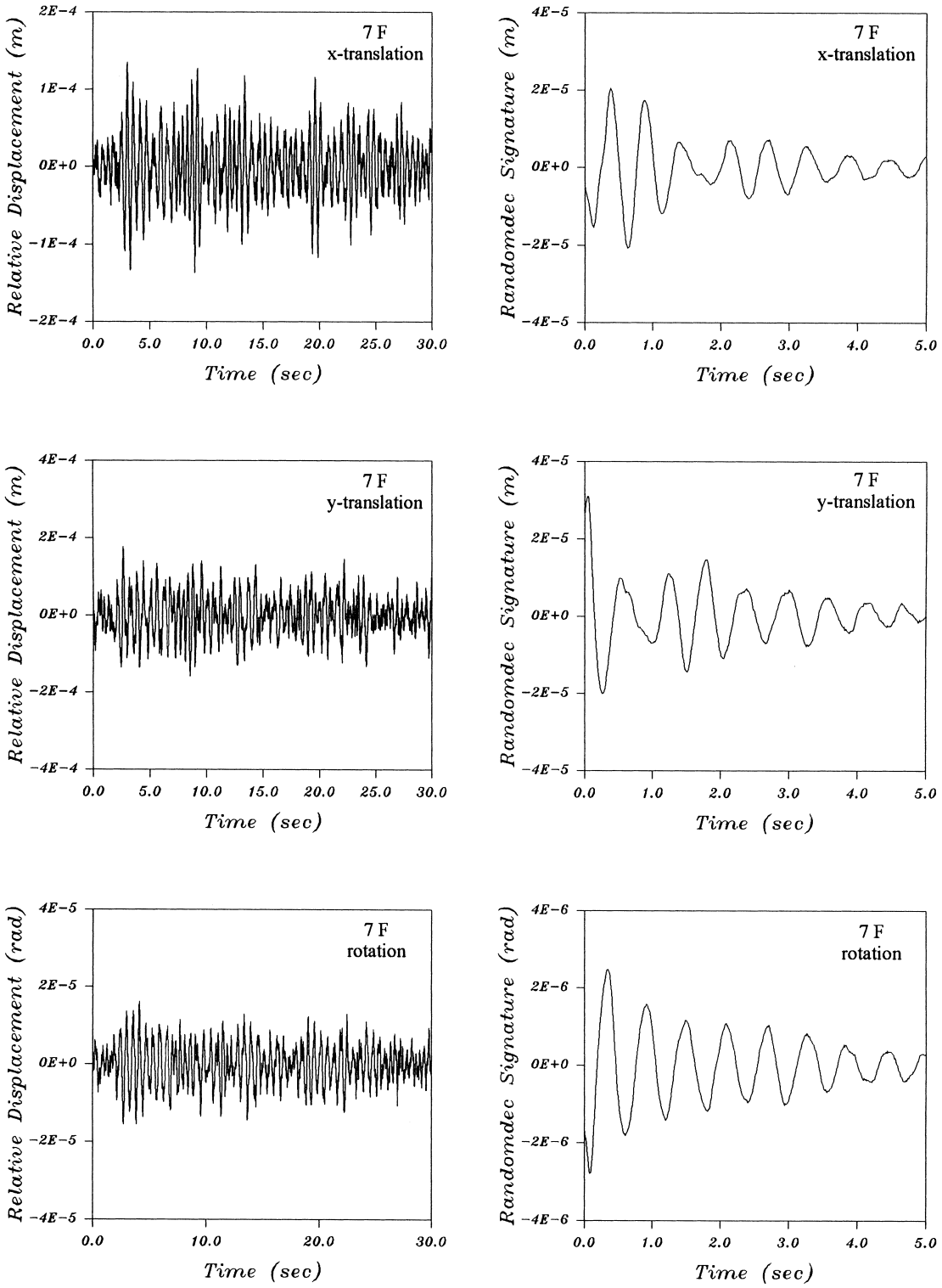

Fig. 4 (*continued*)

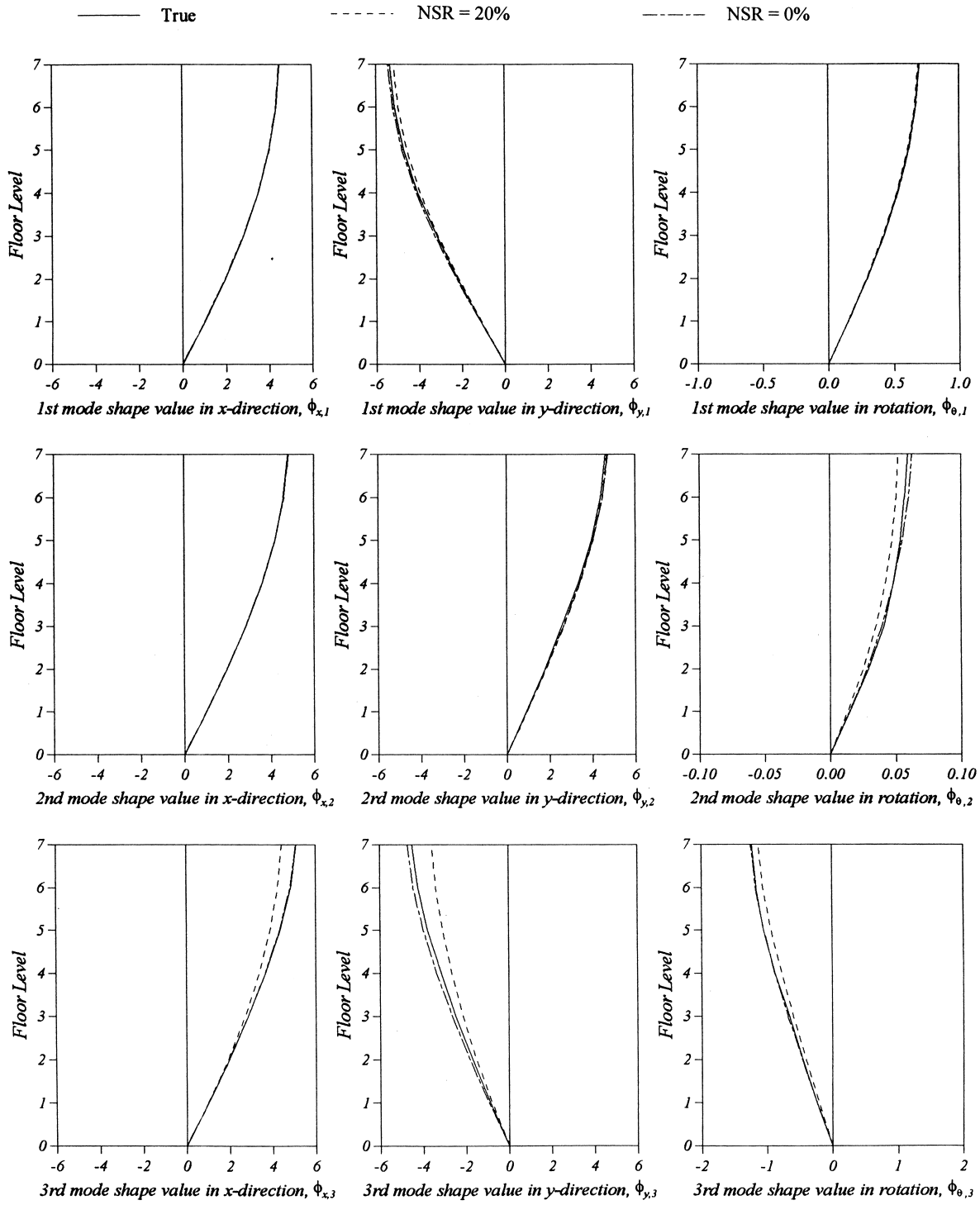

Fig. 5. Calculated vs. true mode shapes of example torsionally coupled building with 1F, 4F, 7F measurements.

the noise-free case, the frequencies identified are almost identical to the true ones. The accuracy of the damping ratio identification is not as good as that for modal frequency and mode shape, but it is still acceptable. The main discrepancy is due to the error for free decay responses obtained using the random decrement method. If true free responses are used, both modal frequencies and damping ratios can be identified very accurately [22]. Moreover, the estimation error increases as the noise level becomes high. As NSR = 20%, the proposed method is still able to identify most of the dominant modal parameters accurately even with highly coupled modes. This identification result is generally adequate for building structures because the total responses are dominated by the first few modes. As expected, case 1 has better results than case 2 because of greater floor response measurements.

The complete first three mode shapes for case 2 calculated by Eqs. (15a) and (15b) are shown in Fig. 5 for NSR = 0% and 20%. There is good agreement between the estimated and true mode shapes. Furthermore, based on the identified modal parameters with NSR = 20%, the predicted relative displacement and absolute acceleration at the sixth floor (unmeasured location) and top floor (measured location) and the base shear in the x-direction for the building under the El Centro (S00E,1940) earthquake are shown in Figs. 6 and 7. Since the dominant modal properties are accurately estimated, so are the dynamic responses. For both cases studied with NSR = 0% and 20%, the peak

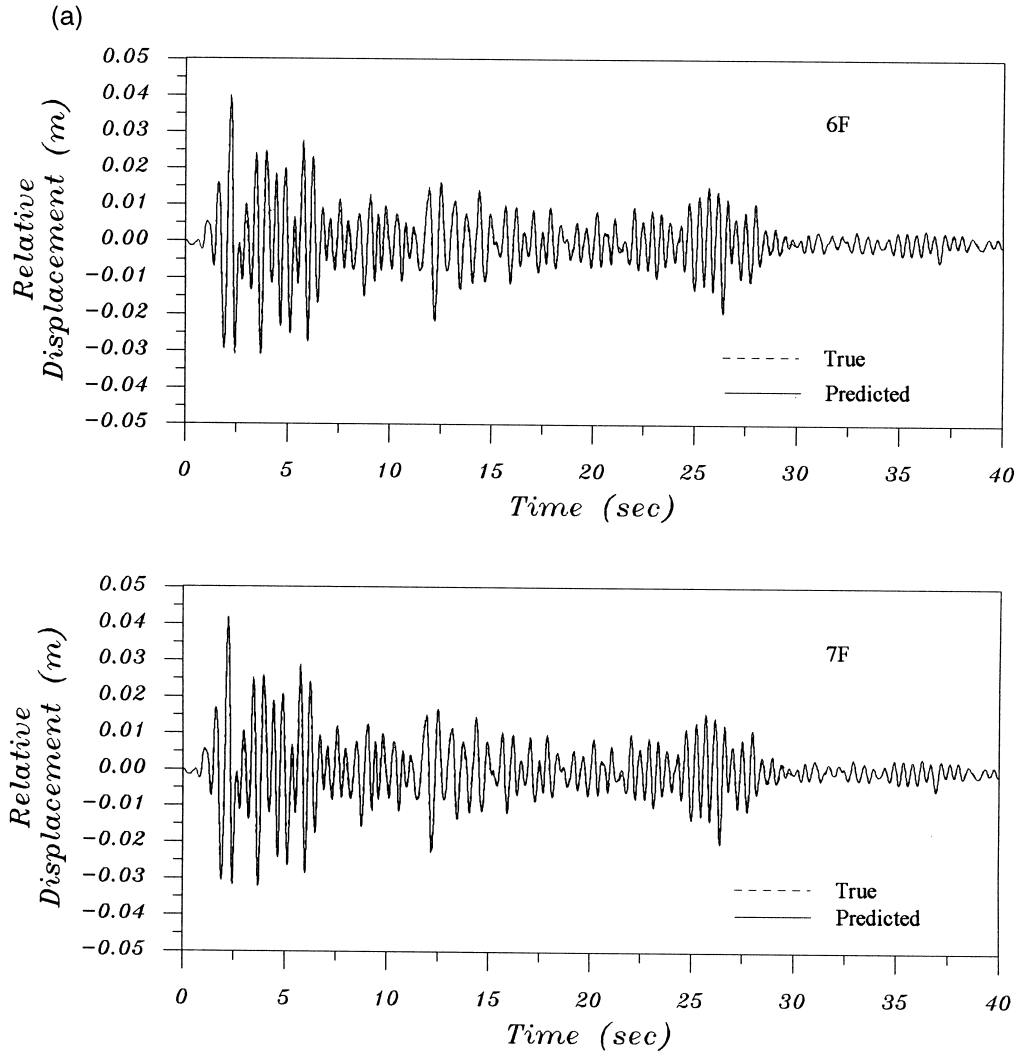

Fig. 6. (a) Predicted 6F and 7F relative displacement in x-direction under El centro earthquake (case 1, NSR = 20%). (b) Predicted 6F and 7F absolute acceleration and base shear in x-direction under El centro earthquake (case 1, NSR = 20%).

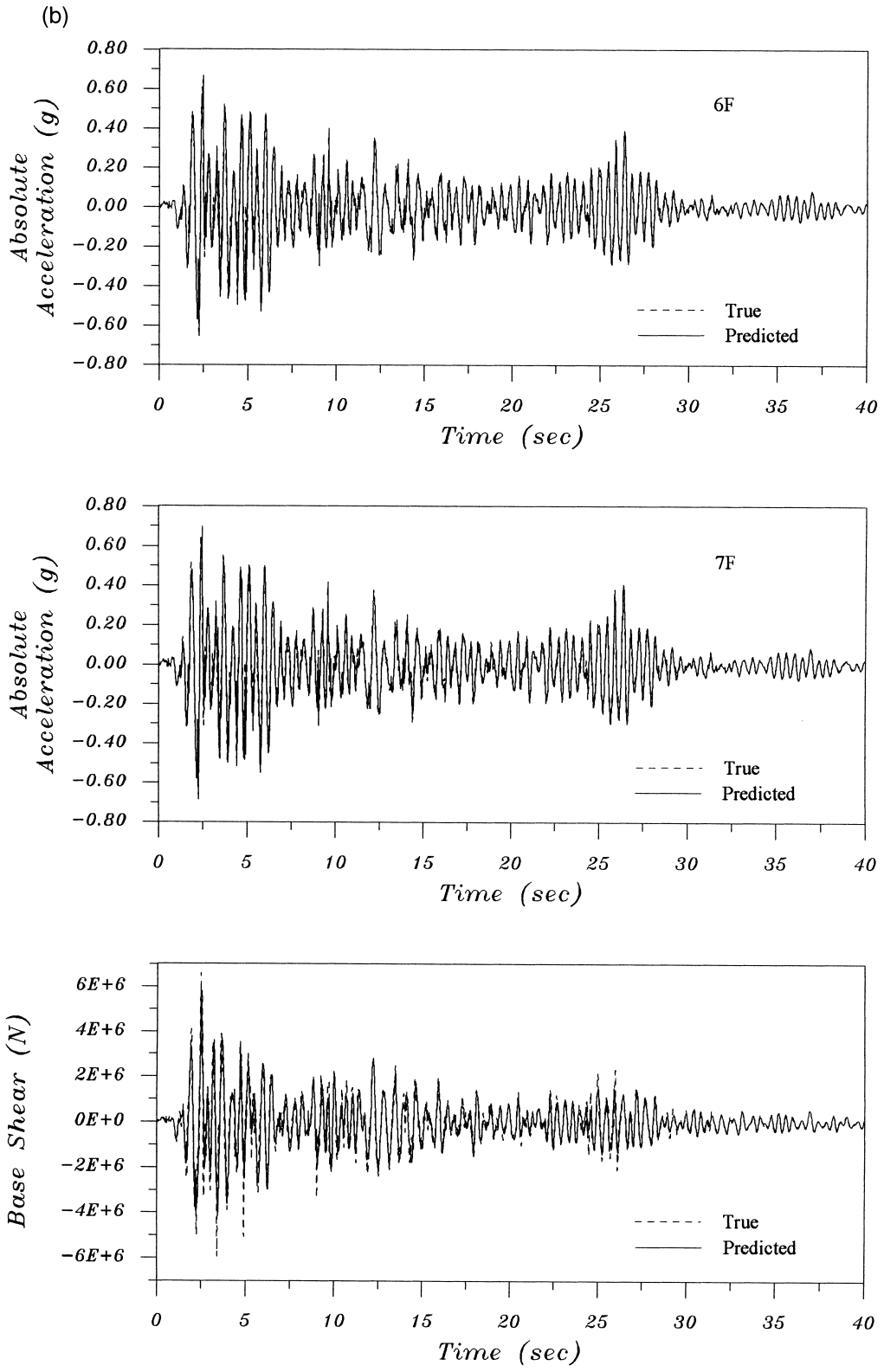

Fig. 6 (*continued*)

Table 3
Peak responses estimation under El centro earthquake

Responses	True	NSR = 0%		NSR = 20%	
		Case 1	Case 2	Case 1	Case 2
x_6 (cm)	4.02	4.06 (+1.0%)	4.06 (+1.0%)	3.95 (−1.7%)	3.95 (−1.7%)
x_7 (cm)	4.18	4.23 (+1.2%)	4.23 (+1.2%)	4.12 (−1.4%)	4.11 (−1.7%)
$\ddot{x}_6$ (g)	0.683	0.679 (−0.6%)	0.679 (−0.6%)	0.660 (−3.4%)	0.665 (−2.6%)
$\ddot{x}_7$ (g)	0.698	0.715 (+2.4%)	0.713 (+2.1%)	0.685 (−1.9%)	0.686 (−1.8%)
x-Base shear (N)	6.6×10^6	6.2×10^6 (−6.1%)	6.2×10^6 (−6.1%)	6.1×10^6 (−7.6%)	6.0×10^6 (−9.1%)

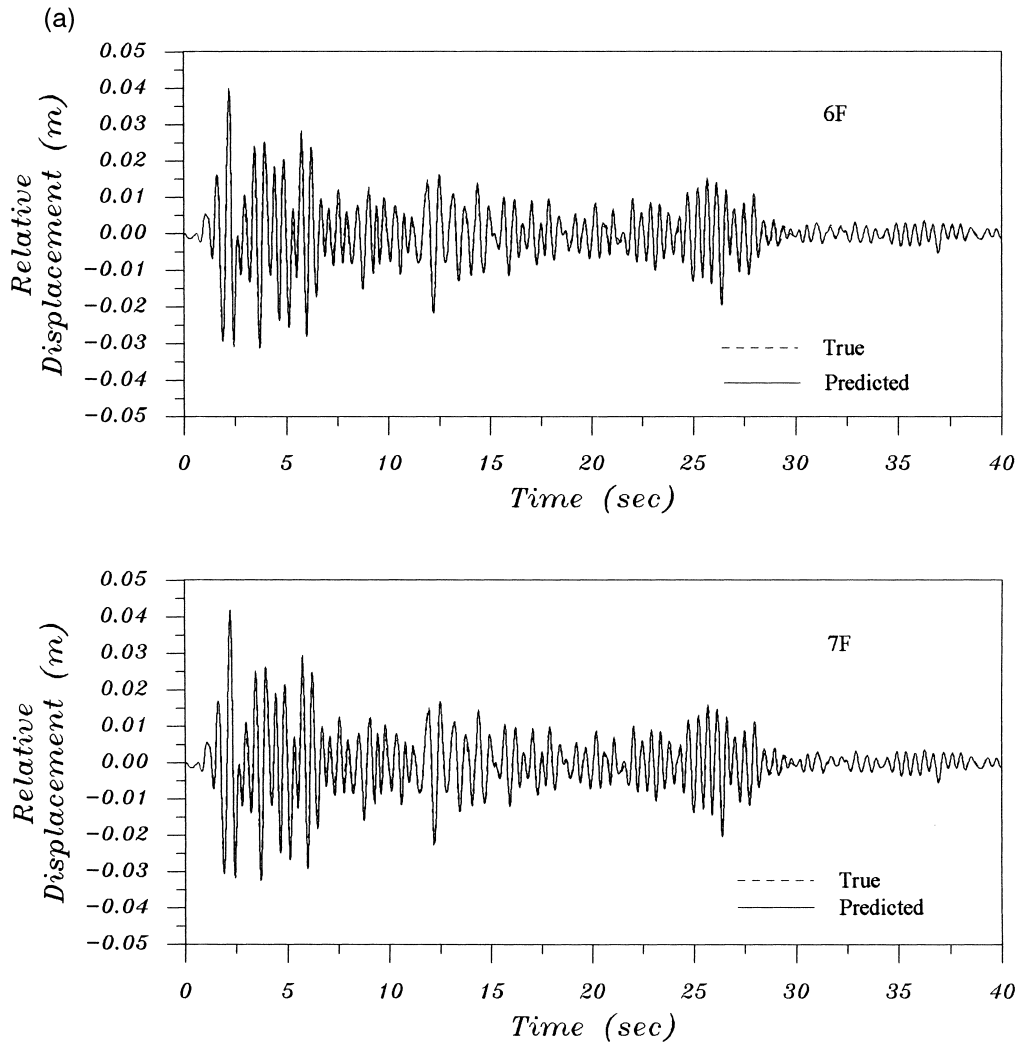

Fig. 7. (a) Predicted 6F and 7F relative displacement in x-direction under El centro earthquake (case 2, NSR = 20%). (b) Predicted 6F and 7F absolute acceleration and base shear in x-direction under El centro earthquake (case 2, NSR = 20%).

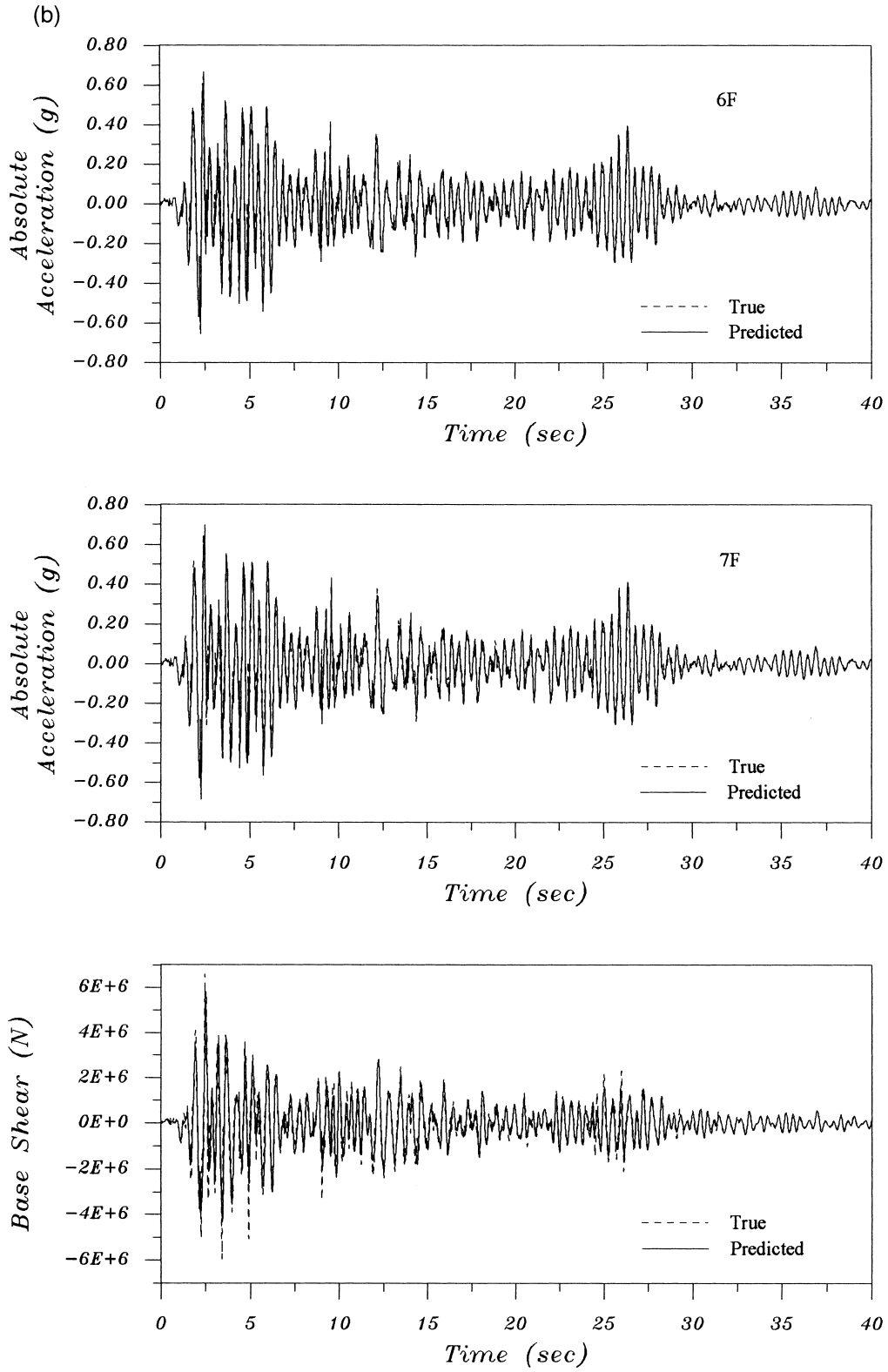

Fig. 7 (*continued*)

Table 4
RMS responses estimation under El centro earthquake

Responses	True	NSR = 0%		NSR = 20%	
		Case 1	Case 2	Case 1	Case 2
x_6 (cm)	0.628	0.613 (−2.4%)	0.605 (−3.7%)	0.658 (+4.8%)	0.669 (+6.5%)
x_7 (cm)	0.656	0.640 (−2.4%)	0.630 (−4.0%)	0.686 (+4.6%)	0.697 (+6.3%)
$\ddot{x}_6$ (g)	0.112	0.108 (−3.6%)	0.105 (−6.3%)	0.119 (+6.3%)	0.122 (+8.9%)
$\ddot{x}_7$ (g)	0.118	0.112 (−5.1%)	0.109 (−7.6%)	0.124 (+5.1%)	0.127 (+7.6%)
x-Base shear (N)	8.8×10^5	8.2×10^5 (−6.8%)	8.2×10^5 (−6.8%)	8.2×10^5 (−6.8%)	8.4×10^5 (−4.5%)

and root-mean-square (RMS) responses at measured and unmeasured locations are listed in Tables 3 and 4. All estimation errors are below 10%. Both estimated response errors increase as the noise level increases. In general, the responses at the measured locations are predicted more accurately than those at unmeasured locations when the measurement noise level is high, as we expected.

7. Conclusions

In this study, a modal parameter identification method, which modifies the Ibrahim time domain technique and the random decrement method was developed to identify the frequencies and damping ratios of general torsionally coupled buildings based on only a few floor response measurements due to ambient vibration excitations. In order to estimate the dynamic responses at each degree-of-freedom, a mode shape interpolation method was developed further to calculate the mode shape values for the locations without measurements. All estimated mode shapes were mutually orthogonal. A study of the theoretical and numerical results indicates that two or more floor response measurements are adequate to identify the dominant modal properties of a general torsionally coupled building. The number of sensors was very small compared to the degree of freedom of the structure. Moreover, for a high-rise building, it is suggested that three (at low, medium and top) floor responses be measured so that the complete dominant modal properties can be accurately obtained. Since the dominant modal frequencies and damping ratios and complete mode shapes are accurately identified even with noise contamination, the seismic responses at both measured and unmeasured locations are thus accurately estimated. A small number of response measurements, no requirement for input excitation measurements and simple on-line calculations make the proposed method favorable for implementation in real buildings.

Acknowledgements

This research was supported in part by National Science Council of the Republic of China under grant No. NSC 84-2621-P-005-003B. This support is greatly appreciated.

References

[1] Kozin F, Natke HG. System identification techniques. Structural Safety 1986;3:269–316.
[2] Luz E, Wallaschek J. Experimental modal analysis using ambient vibration. The International Journal of Analytical and Experimental Modal Analysis 1992;7(1):29–39.
[3] Benzoni G, Gentile C. Two approaches to identify equivalent structural models from earthquake responses. Soil Dynamics and Earthquake Engineering 1993;12:113–25.
[4] Mau ST, Aruna V. Story-drift, shear, and OTM estimation from building seismic records. Journal of Structural Engineering, ASCE 1994;120(11):3368–85.
[5] Toki K, Sato T, Kiyono J. Identification of structural parameters and input ground motion from response time histories. Structural Engineering and Earthquake Engineering, JSCE 1989;6(2):413s–21s.
[6] Wang D, Haldar A. Element-level system identification with unknown input. Journal of Engineering Mechanics, ASCE 1994;120(1):159–76.
[7] Kadakal U, Yüzügüllü Ö. A comparative study on the identification methods for the autoregressive modeling from the ambient vibration records. Soil Dynamics and Earthquake Engineering 1996;15:45–9.
[8] Torkamani MAM, Ahmadi AK. Stiffness identification of a tall building during construction period using ambient tests. Earthquake Engineering and Structural Dynamics 1988;16:1177–88.
[9] Hejal R, Chopra AK. Earthquake analysis of a class of torsionally-coupled buildings. Earthquake Engineering and Structural Dynamics 1989;18:305–23.
[10] Cole Henry A. Method and apparatus for measuring the damping characteristics of a structure. U.S. Patent No. 3-620-069, 1971.
[11] Cole Henry A. On-line failure detection and damping measurement of aerospace structures by random decrement signatures. NASA CR-2205, 1973.

[12] Yang JCS, Caldwell DW. The measurement of damping and the detection of damages in structures by the random decrement method. 46th Shock and Vibration Bulletin 1976:129–136.
[13] Yang JCS, Chen J, Dagalanis NG. Damage detection in offshore structures by the random decrement method. Journal of Energy Resources Technology, ASME 1984;106:38–42.
[14] Caravani P, Watson ML, Thomson WT. Recursive least-square time domain identification of structural parameters. Journal of Applied Mechanics, ASME 1977;44:135–140.
[15] Mickleborough NC, Pi YL. System modal identification using free vibration data. Structural Engineering and Earthquake Engineering, JSCE 1989;6(2):217s–28s.
[16] Shinozuka M, Yun CB. Identification of linear structural dynamical system. Journal of Engineering Mechanics Division, ASCE 1982;108:1317–90.
[17] Ibrahim SR, Mikulcik EC. A method for the direct identification of vibration parameters from the free response. 47th Shock and Vibration Bulletin 1977;part 4:183–198.
[18] Ibrahim SR. Double least squares approach for use in structural modal identification. Journal of Spacecraft and Rockets, AIAA 1986;24(3):499–503.
[19] Ibrahim SR, Pappa RS. Large modal survey testing using the Ibrahim time domain identification technique. Journal of Spacecraft and Rockets, AIAA 1982;19(5):459–65.
[20] Kan CL, Chopra AK. Effects of torsional coupling on earthquake forces in buildings. Journal of Structural Engineering Division, ASCE 1997;103:805–19.
[21] Kan CL, Chopra AK. Elastic earthquake analysis of torsionally-coupled multistorey buildings. Earthquake Engineering and Structural Dynamics 1977;5:395–412.
[22] Lin CC, Ueng JM, Lin PL. System identification of torsionally coupled structures. In: Proceedings of ASME 15th Biennial Conference on Mechanical Vibration and Noise. Boston, USA, vol. 3, Part C. 1995. p. 341–9.
[23] Lin CC, Soong TT, Natke HG. Real-time system identification of degrading structures. Journal of Engineering Mechanics, ASCE 1990;116(10):2258–74.